Inorg. Chem. **2002**, *41*, 2054–2059

Electronic Excited States of $[Au_2(dmpm)_3](ClO_4)_2$ (dmpm = bis(dimethylphosphine)methane)

King Hung Leung, David Lee Phillips,* Zhong Mao, Chi-Ming Che,* Vincent M. Miskowski,* and Chi-Keung Chan

Department of Chemistry and the HKU-CAS Joint Laboratory on New Materials, The University of Hong Kong, Pokfulam Road, Hong Kong

Received October 19, 2001

We present studies of the resonance Raman and electronic luminescence spectra of the $[Au_2(dmpm)_3](ClO_4)_2$ (dmpm = bis(dimethylphosphine)methane) complex, including excitation into an intense band at 256 nm and into a weaker absorption system centered about ~300 nm. The resonance Raman spectra confirm the assignment of the 256 nm absorption band to a $^1(d\sigma^* \rightarrow p\sigma)$ transition, a metal–metal-localized transition, in that ν(Au–Au) and overtones of it are strongly enhanced. A resonance Raman intensity analysis of the spectra associated with the 256 nm absorption band gives the ground-state and excited-state ν(Au–Au) stretching frequencies to be 79 and 165 cm^{-1}, respectively, and the excited-state Au–Au distance is calculated to decrease by about 0.1 Å from the ground-state value of 3.05 Å. The ~300 nm absorption displays a different enhancement pattern, in that resonance-enhanced Raman bands are observed at 103 and 183 cm^{-1} in addition to ν(Au–Au) at 79 cm^{-1} The compound exhibits intense, long-lived luminescence (in room-temperature CH_3CN, for example, $\tau = 0.70$ μs, $\phi_{emission} = 0.037$) with a maximum at 550–600 nm that is not very medium-sensitive. We conclude, in agreement with an earlier proposal of Mason (*Inorg. Chem.* **1989**, *28*, 4366–4369), that the lowest-energy, luminescent excited state is not $^3(d\sigma^* \rightarrow p\sigma)$ but instead derives from $^3(d_{x^2-y^2,xy} \rightarrow p\sigma)$ excitations. We compare the Au(I)–Au(I) interaction shown in the various transitions of the $[Au_2(dmpm)_3](ClO_4)_2$ tribridged compound with previous results for solvent or counterion exciplexes of $[Au_2(dcpm)_2]^{2+}$ salts (*J. Am. Chem. Soc.* **1999**, *121*, 4799–4803; *Angew. Chem.* **1999**, *38*, 2783–2785; *Chem. Eur. J.* **2001**, *7*, 4656–4664) and for planar, mononuclear Au(I) triphosphine complexes. It is proposed that the luminescent state in all of these cases is very similar in electronic nature.

Introduction

There has been great interest in luminescent Au(I) compounds, especially those with intramolecular Au(I)−Au(I) interactions.[1−8] Many photoluminescent studies have been done for Au(I) compounds, and assignment of metal−metal bond emissive excited-state $^3[d\sigma^*p\sigma]$ had been made in many cases.[1] Polynuclear Au(I) compounds with bridging phosphine ligands have been found to have long-lived emissive excited states that are good photoreductants with $E°$ values of about −1.6 to −1.7 V vs SCE[5a,b,f,6a] Some Au(I) compounds exhibit intriguing photochemistry and photoluminescence. For example, the $[Au_2(dppm)_2]^{2+}$ (dppm = bis(diphenylphosphine)methane) complex is a photocatalyst for reductive C−C bond coupling from alkyl halides in the presence of sacrificial electron donors.[5b] Of particular interest is the recent finding that visible luminescence is readily triggered when a two-coordinated gold(I) phosphine complex undergoes substrate binding.[2,4b,5g,h]

* Authors to whom correspondence should be addressed. E-mail (D.L.P.): phillips@hkucc.hku.hk.

(1) Gade, L. H. *Angew. Chem., Int. Ed. Engl.* **1997**, *36*, 1171−1173.
(2) Vickery, J. C.; Olmstead, M. M.; Fung, E. Y.; Balch, A. L. *Angew. Chem., Int. Ed. Engl.* **1997**, *36*, 1179−1181.
(3) Mansour, M. A.; Connick, W. B.; Lachicotte, R. J.; Gysling, H. J.; Eisenberg, R. *J. Am. Chem. Soc.* **1998**, *120*, 1329−1330.
(4) (a) King, C.; Wang, J.-C.; Khan, M. N. I.; Fackler, J. P., Jr. *Inorg. Chem.* **1989**, *28*, 2145−2149. (b) King, C.; Khan, M. N. I.; Staples, R. J.; Fackler, J. P., Jr. *Inorg. Chem.* **1992**, *31*, 3236−3238.
(5) (a) Che, C.-M.; Kwong, H.-L.; Yam, V. W.-W.; Cho, K.-C. *J. Chem. Soc., Chem. Commun.* **1989**, 885−886. (b) Li, D.; Che, C.-M.; Kwong, H.-L.; Yam, V. W.-W. *J. Chem. Soc., Dalton Trans.* **1992**, 3325−3329. (c) Shieh, S.-J.; Hong, X.; Peng, S.-M.; Che, C.-M. *J. Chem. Soc., Dalton Trans.* **1994**, 3067−3068. (d) Tzeng, B.-C.; Cheung, K.-K.; Che, C.-M. *Chem. Commun.* **1996**, 1681−1682. (e) Tzeng, B.-C.; Chan, C.-K.; Cheung, K.-K.; Che, C.-M.; Peng, S.-M. *Chem. Commun.* **1997**, 135−136. (f) Weng, Y.-X.; Chan, K.-C.; Tzeng, B.-C.; Che, C.-M. *J. Chem. Phys.* **1998**, *109*, 5948−5956. (g) Chan, W.-H.; Mak, T. C.-W.; Che, C.-M. *J. Chem. Soc., Dalton Trans.* **1998**, 2275−2276. (h) Fu, W.-F.; Chan, K.-C.; Miskowski, V. M.; Che, C.-M. *Angew Chem., Int. Ed. Engl.* **1999**, *38*, 2783−2785. (i) Che, C−M.; Chao, H.-Y.; Miskowski, V. M.; Li, Y.-Q.; Cheung K.-K. *J. Am. Chem. Soc.* **2001**, *123*, 4985−4991.

10.1021/ic011084v CCC: $22.00
Published on Web 03/21/2002

Metal−metal interactions in dinuclear Au(I) compounds give rise to a strong near-ultraviolet $nd\sigma^* \rightarrow (n+1)p\sigma$ transition that is red-shifted in energy compared to the mononuclear counterparts.[4,5a,9] A well-studied example of dinuclear Au(I) complexes is $[Au_2(dppm)_2]^{2+}$, which displays an intense $5d\sigma^* \rightarrow 6p\sigma$ transition at 297 nm.[4,5a,6a] This compound in the solution phase displays a long-lived photoluminescence at 570 nm that has recently been assigned to come from a solvent/anion exciplex of the $^3[d\sigma^*p\sigma]$ excited state.[5h,7] We have recently applied resonance Raman spectroscopy to investigate the electronic structures of the ground and excited states of dinuclear dibridged Au(I) compounds.[6c,8] With $[Au_2(dcpm)_2]^{2+}$ (dcpm = bis(dicyclohexylphosphine)methane) as a model, we gave the first experimental proof of the $5d\sigma^* \rightarrow 6p\sigma$ electronic transition in dinuclear Au(I)−phosphine compounds and an estimate of the Au(I)−Au(I) bond length change in the initially excited $^1[d\sigma^*p\sigma]$ state.[8] In this paper we report luminescence and resonance Raman investigations on the $[Au_2(dmpm)_3](ClO_4)_2$ (dmpm = bis(dimethylphosphine)methane) compound, which is a prototype example of a dinuclear tribridged $[Au(I)]_2$ compound. We investigate the Au(I)−Au(I) interaction evidenced in these transitions for the $[Au_2(dmpm)_3]^{2+}$ **(1)** tribridged compound and compare it to our previous results for the $[Au_2(dcpm)_2]^{2+}$ **(2)** dibridged compound.

Experimental Section

$[Au_2(dmpm)_3](ClO_4)_2$, [**1**]$(ClO_4)_2$, was prepared according to a literature procedure,[9] and the PF_6^- salt was similarly prepared. Sample solutions of **1** used 5−10 mM concentrations in water solvent. Since the resonance Raman apparatus and methods have been previously detailed,[10] we shall only present a short description. The harmonics of a Nd:YAG laser and their hydrogen Raman shifted laser lines provided the excitation frequencies for the resonance Raman experiments. A lightly focused excitation laser beam photoexcited samples contained in a stirred UV-grade quartz cell. The Raman scattered light was collected using a ∼130° backscattering angle and imaged through a depolarizer and entrance slit of a 0.5 m spectrograph. A 1200 groove/mm ruled grating blazed at 250 nm dispersed the Raman light onto a liquid-nitrogen-cooled CCD detector which collected signal for about 1−2 min before being readout to an interfaced PC computer. Approximately 30−60 of these readouts were summed to obtain the resonance Raman spectrum.

Known solvent Raman bands and Hg lamp emission lines were used to calibrate the vibrational frequencies of the resonance Raman spectra. The resonance Raman spectra were corrected for any leftover sample reabsorption and the response of the detection system as a function of wavelength. The solvent bands, the quartz cell background, and Rayleigh line were subtracted from the experimental resonance Raman spectra using appropriately scaled solvent and quartz background spectra. Segments of the resonance Raman spectra were fit to a baseline plus a sum of Lorentzian bands to determine the Raman band integrated areas.

The absolute resonance Raman cross sections of **1** were measured relative to previously measured Raman cross sections of water solvent bands.[11] The concentrations of the sample solutions were measured spectrophotometrically. The absorption spectra changed by less than 5% during the absolute Raman cross section experiments. The average of a series of measurements at each excitation wavelength was used to determine an absolute cross section value. The absolute resonance Raman cross section exhibited little power dependence (<5%) between 0.1 and 1.5 mW. The maximum molar extinction coefficients for the absorption bands of interest are 18 500 M^{-1} cm^{-1} for the 255.9 nm and 1490 M^{-1} cm^{-1} for the 311.3 nm bands of **1**.[9]

Calculated fits to the absorption and resonance Raman cross sections of **1** employed a time-dependent formalism[12−22] that has been described by us in detail recently.[8] As in our previous work, damping functions were incorporated that were either simple exponential decay or Brownian oscillator dephasing functions.[21]

Electronic emission and emission excitation spectra were measured on a Spex. Emisssion lifetimes employed a setup that has been described elsewhere.[23]

Results

Electronic Absorption. The electronic absorption and MCD spectra of **1** have been reported and analyzed in detail

(6) (a) Yam, V. W.-W.; Lai, T.-F.; Che, C.-M. *J. Chem. Soc., Dalton Trans.* **1990**, 3747−3752. (b) Yam, V. W.-W.; Li, C.-K.; Chan, C.-L. *Angew. Chem., Int. Ed. Engl.* **1998**, *37*, 2857−2859. (c) Cheng, E. C.-C.; Leung, K.-H.; Miskowski, V. M.; Yam, V. W.-W.; Phillips, D. L. *Inorg. Chem*. **2000**, *39*, 3690−3695.

(7) (a) Zhang, H.-X.; Che, C.-M. *Chem. Eur. J.* **2001**, *7*, 4887−4893. (b) Fu, W.-F.; Chan, K−C.; Cheung, K.-K.; Che, C.-M. *Chem. Eur. J.* **2001**, *7*, 4656−4664.

(8) Leung, K.-H.; Phillips, D. L.; Tse, M.-C.; Che, C.-M.; Miskowski, V. M. *J. Am. Chem. Soc.* **1999**, *121*, 4799−4803.

(9) (a) Jaw, H.-R. C.; Savas, M. M.; Rogers, R. D.; Mason, W. R. *Inorg. Chem.* **1989**, *28*, 1028−1037. (b) Jaw, H.-R. C.; Savas, M. M.; Mason, W. R. *Inorg. Chem.* **1989**, *28*, 4366−4369.

(10) (a) Kwok, W.-M.; Phillips, D. L.; Yeung, P. K.-Y.; Yam, V. W.-W. *Chem. Phys. Lett.* **1996**, *262*, 699−708. (b) Kwok, W.-M.; Phillips, D. L.; Yeung, P. K.-Y.; Yam, V. W.-W. *J. Phys Chem. A* **1997**, *101*, 9286−9295. (c) Cheng, Y.-F.; Philips, D. L.; He, G.-Z.; Che, C.-M.; Chi, Y. *Chem. Phys. Lett*. **2001**, *338*, 308−316.

(11) (a) Trulson, M. O.; Mathies, R. A. *J. Chem. Phys.* **1986**, *84*, 2068−2074. (b) Dudik, J. M.; Johnson, C. R.; Asher, S. A. *J. Chem. Phys.* **1985**, *82*, 1732−1740.

(12) Lee, S. Y.; Heller, E. J. *J. Chem. Phys.* **1979**, *71*, 4777−4788.

(13) Myers, A. B.; Mathies, R. A.; Tannor, D. J.; Heller, E. J. *J. Chem. Phys.* **1982**, *77*, 3857−3866.

(14) Tutt, L.; Tannor, D.; Heller, E. J.; Zink, J. I. *Inorg. Chem.* **1982**, *21*, 3858−3859.

(15) Myers, A. B.; Mathies, R. A. *Biological Applications of Raman Spectroscopy*; Wiley: New York, 1987; pp 1−58.

(16) Clark, R. J. H.; Dines, T. J. *Angew. Chem., Int. Ed. Engl.* **1986**, *25*, 131−158.

(17) (a) Doorn, S. K.; Hupp, J. T. *J. Am. Chem. Soc.* **1989**, *111*, 1142−1144. (b) Doorn, S. K.; Hupp, J. T.; Porterfield, D. R.; Campion, A.; Chase, D. B. *J. Am. Chem. Soc.* **1990**, *112*, 4999−5002. (c) Blackbourn, R. L.; Johnson, C. S.; Hupp, J. T.; Bryant, M. A.; Sobocinski, R. L.; Pemberton, J. E. *J. Phys. Chem.* **1991**, *95*, 10535−10537.

(18) (a) Zink, J. I.; Shin, K. S. K. *Adv. Photochem.* **1991**, *16*, 119−214. (b) Hanna, S. D.; Khan, S. I.; Zink, J. I. *Inorg. Chem.* **1996**, *35*, 5813−5819. (c) Bailey, S. E.; Cohan, J. S.; Zink, J. I. *J. Phys. Chem. B* **2000**, *104*, 10743−10749.

(19) (a) Myers, A. B. *Laser Techniques in Chemistry*; Wiley: New York, 1995; pp 325−384. (b) Myers, A. B. *Chem. Rev.* **1996**, *96*, 911−926. (c) Markel, F.; Ferris, N. S.; Gould, I. R.; Myers, A. B. *J. Am. Chem. Soc*. **1992**, *114*, 6208−6219. (d) Kulinowski, K.; Gould, I. R.; Myers, A. B. *J. Phys. Chem*. **1995**, *99*, 9017−9026. (e) Egolf, D. S.; Waterland, M. R.; Kelley, A. M. *J. Phys. Chem. B* **2000**, *104*, 10727−10737.

(20) Yan, Y. J.; Mukamel, S. *J. Chem. Phys.* **1987**, *86*, 6085−6107.

(21) Li, B.; Johnson, A. E.; Mukamel, S.; Myers, A. B. *J. Am. Chem. Soc.* **1994**, *116*, 11039−11047.

(22) (a) Fraga, E.; Webb, M. A.; Loppnow, G. R. *J. Phys. Chem*. **1996**, *100*, 3278−3287. (b) Loppnow, G. R.; Fraga, E. *J. Am. Chem. Soc.* **1997**, *119*, 896−905. (c) Webb, M. A.; Kiser, C. N.; Richards, J. H.; Di Bilio, A. J.; Gray, H. B.; Winkler, J. R.; Loppnow, G. R. *J. Phys. Chem. B* **2000**, *104*, 10915−10920.

(23) Lai, S.-W.; Chan, M. C.-W.; Cheung, T.-C.; Peng, S.-M.; Che, C.-M. *Inorg. Chem*. **1999**, *38*, 4046−4055.

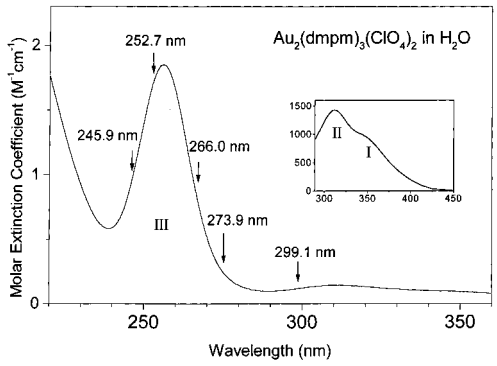

Figure 1. Absorption spectrum of $Au_2(dmpm)_3(ClO_4)_2$ (**1**) in water solution at room temperature with the excitation wavelengths for the resonance Raman experiments shown above the spectrum.

by Mason and co-workers.[9] The room-temperature absorption spectrum is shown in Figure 1. We follow Mason in labeling the three absorption features as bands I−III and analyzing them in D_{3h} symmetry, which is closely approximated by the Au_2P_6 core of **1** in the published crystal structure of the BF_4^- salt.[24]

The intense band III with λ_{max} 256 nm (ϵ 18 500 M^{-1} cm^{-1}) was assigned to the $^1(d\sigma^* \rightarrow p\sigma)$ transition, $^1A_1' \rightarrow {}^1A_2''$, which is dipole-allowed with molecular *z*-polarization. The assignment of a band of $[Au_2(dcpm)_2]^{2+}$ at 277 nm (ϵ 27 000 M^{-1} cm^{-1}) to $^1(d\sigma^* \rightarrow p\sigma)$ is now well-established;[5h,8] $[Au_2(dmpm)_2]^{2+}$ displays an analogous band at 271 nm (ϵ 25 500 M^{-1} cm^{-1}). By comparison, the band of **1** is blue-shifted by 2000−3000 cm^{-1}. It is also broadened; the Gaussian-resolved fwhm of the band is ca. 3000 cm^{-1}, to be compared to 2500 cm^{-1} for the band of $[Au_2(dcpm)_2]^{2+}$.

There are two relatively weak bands, II and I, in the 300−350 nm region, at 311 (ϵ 1490) and 340 nm (ϵ 1070 (sh) M^{-1} cm^{-1}). Mason[9] assigned these bands to dipole-allowed transitions to spin−orbit components of two different triplet states. The $^3(d\sigma^* \rightarrow p\sigma)$ transition, $^1A_1' \rightarrow E'(^3A_2')$, is expected to lie about 5000−6000 cm^{-1} to lower energy of $^1(d\sigma^* \rightarrow p\sigma)$[5h] and may therefore account for one, but not both, of these bands; there is only a single dipole-allowed spin−orbit component of $^3(d\sigma^* \rightarrow p\sigma)$.

Mason proposed that the δ symmetry ($x^2 - y^2$, xy) Au d orbitals should be destabilized for the AuP_3 unit relative to the AuP_2 unit and that $^3(d\delta/\delta^* \rightarrow p\sigma)$ transitions might therefore occur at low energy, contributing to the 300−350 nm absorption region. Specifically, he assigned band I to $^3(d\delta \rightarrow p\sigma)$ and band II to $^3(d\sigma^* \rightarrow p\sigma)$. In strong support of Mason's protocol, McCleskey and Gray subsequently reported the spectrum of $[Au_2(dcpe)_3]^{2+}$ (dcpe = bis-(dicyclohexylphosphino)methane), which has isolated AuP_3 units (Au−Au = 7.05 Å).[25] A band at 370 nm (ϵ 300 M^{-1} cm^{-1}) was assigned to $^3[(d_{xy}, d_{x^2-y^2}) \rightarrow p_z)$. The agreement with band I of **1** is satisfactory.

We should caution that the $^3(d\delta/\delta^* \rightarrow p\sigma)$ excitations of **1** generate a total of eight spin−orbit states in D_{3h} symmetry, including three ($2E' + A_2''$) to which transitions from the ground state are allowed. One specific consequence of this complexity is that weak or forbidden spin−orbit components of $^3(d\delta/\delta^* \rightarrow p\sigma)$ might lie to still lower energy of band I.

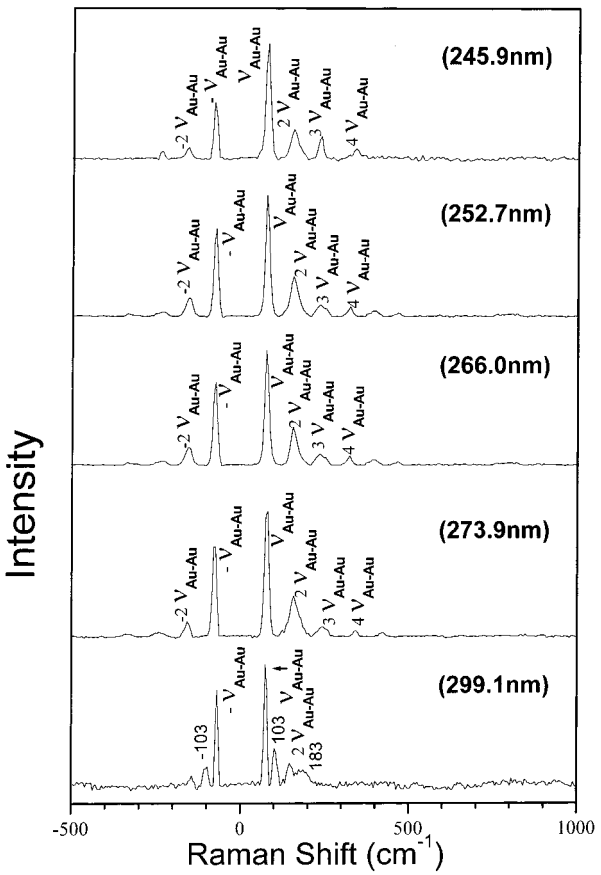

Figure 2. Overview of the resonance Raman spectra of **1** in water solution obtained with 245.9, 252.7, 266.0, 273.9, and 299.1 nm excitation wavelengths. The spectra have been intensity corrected, and the Rayleigh line, glass bands, and solvent bands have been subtracted. The assignments of the prominent Raman bands are indicated.

Resonance Raman. The excitation wavelengths for the resonance Raman experiments are indicated by arrows in Figure 1. Figure 2 shows an overview of the corrected resonance Raman spectra of **1** in aqueous solution. These spectra display the intense fundamental and overtones of a 79 cm^{-1} vibrational mode; except for 299.1 nm excitation, only the 79 cm^{-1} mode is evident in our data. Table 1 gives the data of the resonance Raman bands of **1** in water solution; the corresponding Raman spectrum is depicted in Figure 2. Clearly, the Raman intensities qualitatively track the absorption intensity of band III.

The 79 cm^{-1} frequency is similar to assigned (Au−Au) stretching frequencies for related $[Au_2]$ compounds.[6c,8,26,27] It is puzzling that the value for ν(Au−Au) found here is significantly different from the literature value of 68 cm^{-1}.[26] The latter was obtained for crystalline samples with non-resonant (514.5 nm) excitation. A shift of this magnitude could perhaps be attributed to medium effects, although we do not observe large medium effects upon electronic absorp-

(24) Bensch, W.; Prelati, M.; Ludwig, W. *J. Chem. Soc., Chem. Commun.* **1986**, 1762−1963.
(25) McCleskey, T. M.; Gray, H. B. *Inorg. Chem.* **1992**, *31*, 1733−1734.
(26) Perreault, D.; Drouin, M.; Michel, A.; Miskowski, V. M.; Schaefer, W. P.; Harvey, P. D. *Inorg. Chem.* **1992**, *31*, 695−702.
(27) Harvey, P. D. *Coord. Chem. Rev.* **1996**, *96*, 175−198.

Table 1. Resonance Raman Bands of $[Au_2(dmpm)_3](ClO_4)_2$, [**1**]$(ClO_4)_2$, in Water Solution

band	Raman shift (cm^{-1})	intensity[b] 245.9 nm	252.7 nm	266.0 nm	273.9 nm
-2ν(Au−Au)	−158	7	8	10	9
$-\nu$(Au−Au)	−79	39	49	58	59
ν(Au−Au)	79	100	100	100	100
absolute Raman	expt	1.1×10^{-8}	1.7×10^{-8}	4.7×10^{-9}	9.9×10^{-10}
cross section of	calc[c]	2×10^{-8}	1.7×10^{-8}	6.4×10^{-9}	15×10^{-10}
ν(Au−Au) in $Å^2$/molecule	calc[d]	1.3×10^{-8}	2.7×10^{-8}	5.7×10^{-9}	9.9×10^{-10}
2ν(Au−Au)	160	60	60	61	60
3ν(Au−Au)	240	18	12	9	10
4ν(Au−Au)	316	3	4	4	

[a] Estimated uncertainties are about 2 cm^{-1} for the Raman shifts of (Au−Au) but are systematically larger for overtones. [b] Relative intensities are based on integrated areas of Raman bands. Estimated uncertainties are about 5% for intensities greater than 50, 10% for intensities between 20 and 50, and 20% for intensities below 20. [c] Calculated using the parameters of Table 2A and the exponential decay damping function for solvent dephasing (see text and ref 8 for more details). [d] Calculated using the parameters of Table 2B and the overdamped Brownian oscillator damping function for solvent dephasing (see text and ref 8 for more details).

tion and emission spectra. Alternatively, the literature 68 cm^{-1} feature might actually be due to contamination of the sample with $[Au_2(dmpm)_2]^{2+}$ (ν(Au−Au) = 69 cm^{-1}).[26]

In any case, the 79 cm^{-1} feature is unequivocally attributed to **1** in aqueous solution according to the observed excitation profile. That this is the only vibrational mode enhanced upon excitation into band III suggests that excited-state distortion is restricted to the corresponding normal coordinate. However, we must caution that band III, being molecular *z*-polarized, will specifically enhance the Raman tensor element α_{zz}. Therefore, vibrational modes with intrinsically small values of α_{zz} ("perpendicular" modes), such as ν(Au−P), might exhibit little resonance enhancement even if there are significant excited-state distortions along their normal coordinates. Our identification of the 79 cm^{-1} mode as ν(Au−Au) also requires some qualification. Some degree of mixing of the Au−Au stretching coordinate with δ(P−Au−Au) bending coordinates is to be expected; indeed, increased mixing of this type for three bridging dmpm ligands versus two may account for the higher ν(Au−Au) frequency of **1** relative to $[Au_2(dmpm)_2]^{2+}$.[26] With the data in hand, we cannot treat effects of this type quantitatively. The following attempt at quantitative analysis of resonance enhancement, therefore, ignores these caveats.

The absorption spectrum and the resonance Raman intensities of **1** were simultaneously modeled using time-dependent wave packet calculations to estimate the structural change of the excited electronic state relative to the ground electronic state. We used a simple exponential decay function to mimic the spectral broadening due to solvent dephasing for our first set of computations and an overdamped Brownian oscillator function for our second set of calculations.[8,28] Table 2 gives the best fit simulation parameters for modeling the absorption and resonance Raman data of **1**. Figure 3 compares the calculated and experimental absorption and the resonance Raman intensities for **1** using an overdamped Brownian oscillator function to simulate solvent dephasing. Examination of the figure shows that there appears to be reasonable agreement between the experimental and calculated resonance Raman and absorption intensities.

(28) Leung, K.-H.; Phillips, D. L.; Che, C.-M.; Miskowski, V. M. *J. Raman Spectrosc.* **1999**, *30*, 987−993.

Table 2. Parameters for Simulations of Resonance Raman Intensities and Absorption Spectra of $[Au_2(dmpm)_3](ClO_4)_2$, [1]$(ClO_4)_2$, in Water Solution

A. Parameters for Simulations Using Exponential Decay Damping Function

ground-state vib freq 79 cm^{-1}
excited-state vib freq 165 ± 10 cm^{-1})
$\Delta = 0.65 \pm 0.06$
$E_0 = 38\,880 \pm 100$ cm^{-1}
$M = 1.048 \pm 0.05$ Å
$n = 1.36$
homogeneous broadening, $\Gamma = 2{,}160 \pm 150$ cm^{-1} fwhm
inhomogeneous broadening, $G = 600 \pm 150$ cm^{-1} std dev

B. Parameters for Simulations Using Overdamped Brownian Oscillator Damping Function

ground-state vib freq 79 cm^{-1}
excited-state vib freq 165 ± 10 cm^{-1}
$\Delta = 0.65 \pm 0.06$
$E_0 = 35\,600 \pm 100$ cm^{-1}
$M = 0.895 \pm 0.05$ Å
$n = 1.36$
homogeneous broadening, $\Gamma = 2750 \pm 150$ cm^{-1} fwhm
inhomogeneous broadening, $G = 250 \pm 150$ cm^{-1} std dev
Brownian oscillator $\Lambda = 11.69$ cm^{-1}, $D = 3299$ cm^{-1}

Use of an exponential decay function for solvent dephasing gave very similar results as those shown in Figure 3. Table 1 also shows that there is reasonable agreement between the calculated and experimental absolute resonance Raman cross section measurements for the ν_{Au-Au} fundamental. For the purpose of estimating the structural change of the excited state relative to the ground state, both models give essentially the same best fit parameters. We can use the normal mode displacement parameters listed in Table 2 to obtain an estimate of the Au−Au bond length change of the excited electronic state relative to the ground electronic state. If we assume that the Au−Au vibration is approximately a pure metal−metal stretch, the change in the bond length can be determined from the following formula:[19]

$$q = (\mu\omega/\hbar)^{1/2}(\Delta x) \qquad (1)$$

where q is the dimensionless normal coordinate, μ is the reduced mass of the metal−metal bond, ω is the ground-state vibrational frequency, and Δx is the change in the excited-state bond length relative to its ground-state value. The Au−Au bond length changes by about 0.10 ± 0.01 Å for **1** in the initially $^1[d\sigma^*p\sigma]$ excited state compared to the

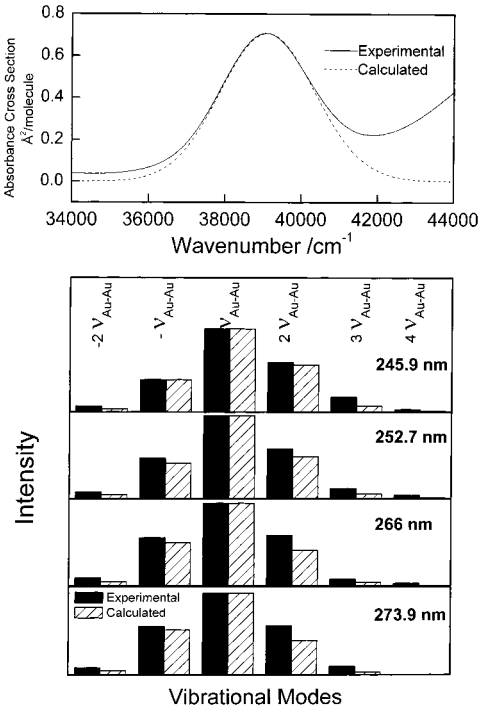

Figure 3. Top: Comparison of the calculated (dashed line) and experimental (solid line) absorption spectra for **1** in water solution. Bottom: Comparison of the calculated (dashed bar) and experimental (solid bar) resonance Raman intensities for 245.9, 252.7, 266.0, and 273.9 nm excitation. The parameters given in Table 2B for **1** were used to calculate the absorption and resonance Raman intensities (the model described in ref 8 and an overdamped Brownian oscillator solvent dephasing function were used for these calculations).

ground-state bond length (3.050(1) Å),[24] and this gives a bond length of ~2.95 Å for the $^1[d\sigma^*p\sigma]$ state of **1**. These bond lengths are somewhat larger than those previously estimated for the dibridged compound **2** (2.92 Å in the ground state and 2.81 Å for the $^1[d\sigma^*p\sigma]$ state).[8] The tribridged compound **1** has bond lengths for both the ground and excited states that are a little over 0.1 Å longer than those in the dibridged compound **2**. The ground- and excited-state frequencies for **1** (79 and 165 cm^{-1}, respectively) are similar to those found for **2** (88 and 175 cm^{-1}, respectively). The large increase in the excited-state Au−Au stretch vibrational frequency and the significant bond length change in the excited state relative to the ground state for **1** are consistent with the assignment of the 256 nm absorption band to a $5d\sigma^* \rightarrow 6p\sigma$ electronic transition. This is very similar to the situation found for **2**.[8] Changing from a dibridged Au dimer system (**2**) to a corresponding tribridged Au dimer compound (**1**) appears to moderately lengthen the Au−Au bond in the ground and excited states while leading to a somewhat larger change in the vibrational frequency (and corresponding calculated "diatomic" force constant) upon excitation from the ground electronic state to the initially excited electronic state. The 9 cm^{-1} downshift in the ground state $\nu(Au_2)$ frequency for **2** versus **1** is entirely consistent with the 2000 cm^{-1} upshift in the energy of the $^1[d\sigma^* \rightarrow p\sigma]$ transition that is observed for **1** versus **2**; that is, the $^1[d\sigma^* \rightarrow p\sigma]$ transition of **1** is a little closer to the monomer $^1[d_{z^2} \rightarrow p_z]$ transition.

Table 3. Structural and Spectroscopic Data for Selected Au_2 Compounds

compd[a]	ν(Au−Au) (cm^{-1})	F(Au−Au) (mdyne/Å)	ln F(Au−Au)	r(Au−Au) (Å)
$Au_2(dmb)(CN)_2$	36	0.075	−2.59	3.536
$Au_2(tmb)Cl_2$	50	0.14	−1.97	3.301
$Au_2(ylide)_2$	64	0.24	−1.43	2.977
$[Au_2(dmpm)_3](PF_6)_2$	68	0.27	−1.31	3.045
$[Au_2(dmpm)_2](PF6)_2$	69	0.28	−1.27	3.044
$[Au_2(dmpm)_2]Cl_2$	71	0.29	−1.24	3.010
$Au_2(ylide)_2Cl_2$	162	1.98	0.68	2.597
$Au_2^+(^2\Sigma_u^+)$	149	1.29	0.25	2.582
$Au_2(^3\Sigma_u^+)$	142	1.18	0.165	2.568
$Au_2(^1\Sigma_g^+)$	180	1.88	0.63	2.520
$Au_2(^1\Sigma_u^+)$	191	2.11	0.75	2.472
$[Au_2(dmpm)_3]^{2+}$ (**1**)	79	0.362	−1.016	3.050[b]
$[Au_2(dmpm)_3]^{2+}$ (**1**),	165[c]	1.58	0.457	2.95[c]
excited-state $^1[d\sigma^*p\sigma]$	135[e]	1.06	0.056	2.95[c]
$[Au_2(dcpm)_2]^{2+}$ (**2**)	88	0.449	−0.80	2.92[b]
$[Au_2(dcpm)_2]^{2+}$ (**2**)	175[d]	1.777	0.57	2.81[d]
excited-state $^1[d\sigma^*p\sigma]$	145[e]	1.220	0.20	2.81[d]

[a] The values for the first 11 compounds of this table come from Table 8 of refs 27 and 28 which also lists the original references from which these values can be found. [b] Value from ref 24. [c] Values from resonance Raman intensity analysis of this work. [d] Values from ref 8. [e] Possible value if resonance Raman intensity analysis overestimates excited-state frequency by 30 cm^{-1}.

Inspection of the simulation parameters in Table 2 for **1** shows that a substantial amount of inhomogeneous broadening is required to simultaneously fit the absolute Raman cross section and the absorption bandwidth. In our previous work on **2**,[8] the inhomogeneous broadening could be largely attributed to a distribution of weak or nascent solvent/anion complexes as there is excellent evidence for strongly bound exciplexes of **2**.[5h] There is no similar evidence currently available for complexation with the excited states of **2**, but the axial sites are open and, conceivably, axial solvent or anion interactions may occur.

It is interesting to compare the Au−Au bond distances and force constants for the ground and excited states of **1** and **2** with previous studies of dinuclear Au compounds.[26,27] Table 3 lists the Au−Au stretch vibrational frequencies, force constants, and bond lengths for the ground and $^1[d\sigma^*p\sigma]$ excited states of **1** and **2** and the ground state of several other compounds, and these are also compared to Harvey's Au−Au bond distance force constant correlation in Figure S-1 of the Supporting Information.[26,27] We have performed additional calculation involving constraints related to Harvey's Au−Au bond distance force constant correlation (see Figure S-2 and Table S-1 in the Supporting Information). The results of these calculations were consistently in poorer agreement with experiment (especially for the intensity in the Raman overtone bands) than those we have presented in Figure 3.

The absorption spectra of **1** and **2** display one distinct difference, other than the blue-shift of the $^1[d\sigma^* \rightarrow p\sigma]$ band for **2**, which is that there are two relatively weak bands ($\epsilon \sim 10^3\ M^{-1}\ cm^{-1}$) near 300 nm for **1** versus one for **2**. Mason and co-workers[9] analyzed this situation in detail and concluded that one of the weak ~310 nm bands of **1** was attributable to the $^3[d\sigma^* \rightarrow p\sigma]$ transition, analogous to **2**, but that the other was due to a transition $^3[d\delta/\delta^* \rightarrow p\sigma]$,

Table 4. Photophysical Data for **1**$(ClO_4)_2$[a]

solvent	λ_{max}(emission) (nm)	τ (μs)	ϕ[f]
4:1 MeOH/EtOH	585	0.7	0.036
4:1 MeOH/EtOH[b]	579	12.8	c
solid	558	7.0[d]	c
solid[e]	556	6.8	c
H_2O	604	0.94	0.043
CH_3CN	580	0.70	0.037

[a] $T = 300$ K except as noted. [b] $T = 77$ K. [c] Not measured. [d] A value of 13 ms was determined at $T = 15$ K. [e] PF_6^- salt. [f] Emission quantum yield.

where dδ/δ* are derived from d_{xy,x^2-y^2} orbitals and are destabilized in **1** versus **2** by the increased σ-donation of three versus two equatorial phosphine donor ligands.

We accept Mason's assignments and assume that they have something to do with the peculiarities of our 299.1 nm resonance Raman spectra. Excitation at 299.1 nm yields a RR spectrum that is substantially different from those at the shorter wavelength (see Figure 2). Unlike **2**, where off-resonance spectra at 299.1 nm were simply a diminuted version of the resonance spectra,[8] those for **1** show several new features, in particular, bands at 103 and 183 cm^{-1}. ν(Au−Au) (and overtones of it) remains a strong feature, but this is possibly due to preresonance with the 256 nm band. The 183 cm^{-1} band can be assigned to a combination of the 103 and 88 cm^{-1} bands, but it is extremely broad and, hence, may encompass more than one vibrational feature. We suggest that these resonance-enhanced (the concentration is too low to allow nonresonance Raman to be significant) Raman lines may involve Au−P motions (perhaps, bending for the 103 cm^{-1} band and stretching for the ∼183 cm^{-1} band). This would be consistent with Mason's assignments, as $\delta/\delta^* \rightarrow p\sigma$ excitations should result in excited-state decreases in Au−P bond lengths, just as they have been inferred to do so for the analogous $d_{xy,x^2-y^2} \rightarrow p_z$ excitation of the mononuclear planar Au(I) tris(phosphine) centers.[25] However, the resonance condition is very marginal for absorption bands with ϵ only ∼1000 M^{-1} cm^{-1}, so no quantitative analysis was attempted for the 299.1 nm data.

Electronic Emission. Compound **1**$(ClO_4)_2$ exhibits intense, broad (fwhm ca. 3500 cm^{-1}) yellow luminescence both as a solid and in degassed solution. The solution excitation spectrum establishes the authenticity of the emission (see Figure S-3). Photophysical parameters are summarized in Table 4. A modest medium sensitivity is observed, the emission maximum varying over a range of ca. 1500 cm^{-1}.

Our observations for **1** are in distinct contrast to the behavior of $[Au_2(dcpm)_2]^{2+}$, as well as that of $[Au_2(dmpm)_2]^{2+}$ (unpublished work). The bis(diphosphine)-bridged $[Au(I)]_2$ complexes exhibit visible luminescence, like **1**, in fluid solution but in rigid media (solid or glass) exhibit long-lived near-UV emission characteristic of the $^3(d\sigma^* \rightarrow p\sigma)$ excited state.[5h,7] The visible emissions of **2** are attributable to solvent/anion exciplexes, but those of **1** are evidently intrinsic.

Conclusion

Our resonance-Raman results show that the assignment of the 256 nm absorption band of **1** to the $^1(d\sigma^* \rightarrow p\sigma)$ transition is correct. The excitation clearly has metal−metal character, as indicated by the strong $\nu(Au_2)$ enhancement and, particularly, by the ca. 0.1 Å decrease in d(Au−Au) that we calculate for this excited state from the wavelength dependence of the absolute resonance-Raman scattering cross sections.

The energy of the assigned $^1(d\sigma^* \rightarrow p\sigma)$ transition is reasonable. The correlating $^1(nd \rightarrow (n+1)p)$ transitions of mononuclear $[Au(PR_3)_2]^+$ are observed in the region of 205−210 nm,[29] indicating a substantial stabilization of $^1(d\sigma^* \rightarrow p\sigma)$ by excited-state gold−gold interaction. It is noteworthy that the visible electronic emission spectra of **1** and **2** in fluid media and planar 3-coordinate mononuclear Au(I) complexes[4b,25,30] are all very similar. We propose that these emissions all derive from monomer-like planar 3-coordinate $^3(d_{x^2-y^2,xy} \rightarrow p_z)$ excited states that are only weakly perturbed by Au−Au interaction in the dinuclear complexes. It is only for **2** and closely related complexes in rigid media (suppressing exciplex formation) that true metal−metal luminescence from $^3(d\sigma^*p\sigma)$ excited states can be observed,[5h] presumably because "in-plane" excited states derived from $d_{x^2-y^2,xy} \rightarrow p_z$ excitations lie at higher energy for lower coordination numbers at Au(I).

Acknowledgment. This work was supported by grants from the Committee on Research and Conference Grants (CRCG), the Hong Kong University Foundation, the Research Grants Council (RGC) of Hong Kong (HKU 7298/99P to C.M.C. and HKU 474/94P to D.L.P.), the Hung Hing Ying Physical Sciences Research Fund, and the Large Items of Equipment Allocation 1993-94 from the University of Hong Kong. C.M.C. is the recipient of the HKU Distinguished Research Award (2000). D.L.P. is the recipient of a HKU Young Outstanding Researcher Award (2000).

Supporting Information Available: A table of resonance Raman simulation parameters for three cases of parameters constrained to values consistent with Harvey correlation and comparison of the computed and experimental Raman cross sections (Table S-1), a plot of r(Au−Au) versus ln F(Au−Au) for the 11 compounds and the excited states of **1** and **2** listed in Table 3 (Figure S-1), comparison of calculated and experimental absorption spectra and resonance Raman intensities for the three cases of parameters given in Table S-1 (Figure S-2), and the emission spectrum of **1**$(ClO_4)_2$ (Figure S-3). This material is available free of charge via the Internet at http://pubs.acs.org.

IC011084V

(29) Savas, M. M.; Mason, W. R. *Inorg. Chem.* **1987**, *26*, 301−307.
(30) Forward, J. M.; Assefa, Z.; Fackler, J. P., Jr. *J. Am. Chem. Soc.* **1995**, *117*, 9103−9104.